arXiv:nucl-th/9807065v1 24 Jul 1998

IFUP-TH 34/97

DYNAMICAL EFFECTS ON THE PARALLEL MOMENTUM DISTRIBUTIONS OF NEUTRONS FROM HALO BREAKUP

Angela Bonaccorso$^+$ and David M.Brink†

$^+$*Istituto Nazionale di Fisica Nucleare, Sezione di Pisa, 56100 Pisa, Italy,*

E-mail: BONACCORSO@AXPIA.PI.INFN.IT

† *Dipartimento di Fisica, Università di Trento, 38050 Povo, Italy, and*

ECT, 38050 Villazzano, Trento, Italy,* E-mail: BRINK@SCIENCE.UNITN.IT

Abstract

In this paper we study the energy spectra and related parallel momentum distributions of the neutrons from the breakup of ^{11}Be. Earlier papers on transfer to the continuum reactions have shown that the breakup amplitude reduces to a simple eikonal approximation in the limit of weakly bound projectiles. The aim is to establish a reliable method to obtain information on the structure of the halo from the experimental results which depend on the reaction mechanism. Theoretical results for the widths of the parallel momentum distributions and for the total breakup cross section are compared to recent experimental data.

PACS number(s):25.70.Hi, 21.10Gv,25.60Ge,25.70Mn,27.20+n

I. INTRODUCTION

The fact that energy spectra of particles emitted to the continuum from a nucleus in a nuclear reaction bear some relation with their original momentum distribution has been known and studied for many years [1]- [15] and the form and widths of the energy distribution have been related to the original momentum distribution of the emitted particle in the projectile. Reactions with final state having a neutron in the continuum have been studied in detail by us [16]- [21] and we arrived at the conclusion that there were dynamical effects modifying the original distributions [20]. An important consequence of our approach is that it is the component of the momentum distribution of the breakup neutron in the projectile parallel to the direction of relative motion that is responsible for the form of the energy distribution. This is in contrast to the results given in refs. [1,2,11] where it is the total momentum distribution of the neutron in the target which is important while it is similar to the approaches of [10,12,13]. Ideas and techniques very similar to ours have been recently used in [12] to the study of halo breakup.

We will not repeat derivations given in earlier papers but, in order to make this paper more self contained, we will describe the physical motivation of our approach and the underlying assumptions. Our aim is to show that halo breakup can be studied by using simple analytical formulae which are more general and more accurate than the eikonal forms and reduce to them in the limit of zero initial binding energy. The main difference between the present approach and the eikonal approach comes from the fact that the rescattering of the breakup neutron on the target is calculated by the optical model. On the other hand the use of the semiclassical approximation for the relative motion of the two ions, discussed in the following, makes our method computationally much simpler than the DWBA type of approach used for example in Ref. [15].

One basic assumption is the masses of the target and projectile core are large compared with that of the neutron. Another is that the relative motion of the projectile and target can be treated classically. For the high energy reactions described in the present paper we assume that the center of the projectile core moves on a straight line path with constant velocity and with a particular impact parameter relative to the target. In our reference frame the target is at rest. We represent the interaction of the neutron with the projectile core by a single particle potential moving with the projectile velocity, and its interaction with the target by an optical potential. We use an approximate solution of the time dependent Schrödinger equation for the neutron moving under the influence of these two potentials with the initial condition that it is bound in a particular state in the projectile. The theory presented in Section II yields an expression Eq.(2.2) for the momentum (or energy) distribution of the neutron in the final state as a function of the impact parameter. The cross-section is obtained by integrating over the impact parameter.

One consequence of the use of a straight line trajectory with constant velocity for the motion of the projectile core relative to the target is that the theory does not satisfy the overall energy and center of mass momentum conservation conditions. The neutron receives energy from the time dependent potential fields associated with the relative motion of the target and projectile. For a given neutron final energy and momentum the overall energy and momentum conditions have to be put in by hand. We discuss this point at the beginning of the next section. The use of straight line trajectories neglects Coulomb deflections. This is a good approximation for light targets and projectiles and high incident energies. We have discussed corrections for Coulomb deflections in earlier papers [22] on transfer to bound states. The same methods could be used for breakup where necessary.

II. THE BREAKUP CROSS SECTION

The breakup theory presented in this paper evolved from a theory for neutron transfer to resonance states of the target [16]. In that case the final neutron energy ε_f was the energy of the neutron resonance in the target. Thus in the present work ε_f is the energy of the neutron relative to the target in the final state. For elastic breakup this is the same as the final laboratory energy of the neutron if the target recoil kinetic energy is neglected. In the case of compound nucleus formation ε_f is the excitation energy of the compound state above the neutron threshold in the residual nucleus. In the case of inelastic scattering it is the energy of the breakup neutron before it scatters from the target. This is equivalent to the sum of the excitation energy of the target final state and the final neutron energy relative to the target. If the target recoil kinetic energy is neglected the final kinetic energy E_f of the ejectile is given by the energy conservation condition

$$E_f - E_{inc} = Q = \varepsilon_i - \varepsilon_f, \tag{2.1}$$

where E_{inc} is the initial incident energy of the projectile in the laboratory, Q is the reaction Q-value given by $Q = \varepsilon_i - \varepsilon_f$ and ε_i is the initial neutron binding energy in the projectile. The projectile is supposed to remain in its ground state after the transfer. With this approximation Eq.(2.1) relates ε_f to the energy loss spectrum of the ejectile. It is not possible to calculate corrections due to target recoil within the present theory because of the three-body character of the final state. This should be done to discuss experiments in which a full kinematical reconstruction is made. However such experiments are not available at present.

The starting point of the present paper is the expression for the energy distribution of the breakup neutron given in Eq.(2.2) which was derived in [16]. It is obtained by working in the target reference frame. The projectile-target relative motion is treated semiclassically by using a trajectory of the center of the projectile relative to the center of the target $\mathbf{s}(t) = \mathbf{d} + \mathbf{v}t$ with constant velocity v in the z-direction and impact parameter $\mathbf{d}$ in the xy-plane.

Eq.(2.2) gives the neutron transfer probability from a definite single particle state of energy ε_i, momentum $\gamma_i = \sqrt{-2m\varepsilon_i}/\hbar$, and angular momentum l_i in the projectile to a final continuum state of energy ε_f, momentum $k_f = \sqrt{2m\varepsilon_f}/\hbar$ within an interval $d\varepsilon_f$. It is the sum of the transfer probabilities to each possible final l_f-state in the energy bin $d\varepsilon_f$

$$\frac{dP}{d\varepsilon_f} \approx \Sigma_{l_f}(|1 - \langle S_{l_f}\rangle|^2 + 1 - |\langle S_{l_f}\rangle|^2)B(l_f, l_i). \tag{2.2}$$

The physical interpretation is that the projectile brings up the neutron which is scattered into a continuum state by the target. The interaction of the neutron with the target is represented by the S-matrix for scattering of a free neutron by the target nucleus.

In the derivation of Eq.(2.2) in [16] the neutron final state was taken as a scattering wave function of energy ε_f, including all possible neutron-target final state interactions, and $\langle S_{l_f}\rangle$ is the optical model, energy averaged S-matrix which describes the re-scattering of the neutron on the target [18]. In Ref. [17] it was shown that the first term of Eq.(2.2), proportional to $|1-\langle S_{l_f}\rangle|^2$, gives the neutron elastic breakup spectrum while the second term proportional to the transmission coefficient $T = 1 - |\langle S_{l_f}\rangle|^2$ gives the absorption spectrum. This term contains contributions from inelastic scattering of the breakup neutron by the target nucleus and also from compound nucleus formation.

The factor $B(l_f, l_i)$ is an elementary transfer probability which depends on the details of the initial and final states, on the energy of relative motion and on the distance of closest approach d between the two nuclei. Its explicit expression reads:

$$B(l_f, l_i) = \frac{1}{2}\left(\frac{\hbar}{mv}\right)^2 \frac{m}{\hbar^2 k_f}(2l_f + 1)P_{l_f}(X_f)|C_1|^2 \frac{e^{-2\eta d}}{2\eta d} P_{l_i}(X_i), \tag{2.3}$$

where the arguments of the Legendre polynomials P_{l_i} and P_{l_f} are respectively $X_i = 1 + 2(k_1/\gamma_i)^2$ and $X_f = 2(k_2/k_f)^2 - 1$. Also $k_1 = -(\varepsilon_i - \varepsilon_f + \frac{1}{2}mv^2)/(\hbar v)$ and $k_2 = -(\varepsilon_i - \varepsilon_f - \frac{1}{2}mv^2)/(\hbar v)$ are the z-components of the neutron momentum in the initial and final state respectively. η is the modulus of the transverse component of the neutron momentum. It is conserved during the breakup process and in fact it can be given both in terms of the initial or final neutron parameters as $\eta^2 = k_1^2 + \gamma_i^2 = k_2^2 - k_f^2$. $mv^2/2$ is the incident energy per nucleon at the distance of closest approach d for the ion-ion collision.

In the case of a weakly bound projectile it is possible to obtain much simpler expressions for the elastic breakup and absorption probabilities. In fact k_2 which is the k_z component of the neutron momentum with respect to target, in the limit of a very small initial binding energy takes the value $k_2 \approx k_f$. Then the Legendre polynomial $P_{l_f} \approx 1$ since its argument is very close to one. By introducing the classical angular momentum $\lambda = k_f b$ and $2l_f + 1 = 2(l_f + 1/2) = 2\lambda$ in Eq.(2.2) we can replace the sum over the final angular momenta with an integral over the neutron impact parameters b with respect to the target. Also when the neutron rescattering on the target takes place at relatively high energy ($\varepsilon_f \simeq \frac{1}{2}mv^2$), the phase shift in $S_{l_f} = e^{2i\delta_{l_f}}$ can be approximated by the eikonal form using a phenomenological optical potential such that $S_{l_f} \approx e^{-i\chi(b)}$ and $\chi(b) = \frac{1}{\hbar v}\int_{-\infty}^{\infty} V_2(x, y, z')dz'$ where V_2 is a complex potential whose real and imaginary strengths are negative. Then

$$\frac{dP(d)}{d\varepsilon_f} \approx \frac{m}{\hbar^2 k_f}\int_0^{\infty} bdb\left[|(1 - e^{-i\chi(b)})|^2 + 1 - |e^{-i\chi(b)}|^2\right]|\tilde{\psi}_1(d, k_1)|^2, \tag{2.4}$$

which is the product of the free neutron elastic (plus absorption) cross section, by the modulus square of the initial state momentum distribution along the relative motion direction, for a fixed value of the distance d. The more accurate expression used in [21] corresponds to replacing the d in the wave function $\tilde{\psi}_1$ in the last term of Eq.(2.4) by $|\mathbf{b} - \mathbf{d}|$. It can be obtained by approximating P_{l_f} by a Bessel function, $P_{l_f}(X_f) \approx I_0(2\eta l_f/k_f) = I_0(2\eta b)$. The total breakup probability is the sum of an elastic plus absorptive term because the full final state wave function contains a S-matrix which is unitary. In [21] instead we started directly from an eikonal wave function for the neutron final state and we obtained only the elastic breakup term since in that case the S-matrix was not unitary. The results discussed in this paper were obtained with Eq.(2.2), but Eq.(2.4) is very useful to get an insight into the physics involved in halo breakup.

In Eq.(2.4) $|\tilde{\psi}_1|^2$ is the initial state momentum distribution [21]

$$|\tilde{\psi}_1(d,k_1)|^2 = \frac{1}{2l_i+1}\Sigma_{m_i}|\tilde{\psi}_{l_im_i}(d,k_1)|^2 \approx |C_1|^2\,\frac{e^{-2\eta d}}{2\eta d}P_{l_i}(X_i), \tag{2.5}$$

C_1 is the asymptotic normalization constant of the initial wave function. The energy distribution of the final neutron has its main origin in the k_1 dependence of $\tilde{\psi}_1$.

The relation between the energy distribution probability and cross section is given by

$$\frac{d\sigma}{d\varepsilon_f} = C^2 S\int_0^\infty d^2\mathbf{d}\frac{dP(d)}{d\varepsilon_f}P_{el}(d) \tag{2.6}$$

as in Eq.(7) of [21]. $P(\varepsilon_f,d)$ is given by Eq.(2.2). $P_{el}(d) = |S_{ct}|^2$ is the ion-ion elastic scattering probability given by the modulus square of the projectile core-target S-matrix. The above factorized form of the neutron-target scattering by the core-target scattering has been used already in several papers on halo breakup , as Ref. [10,13,14,21] and and it is well known to hold for peripheral reactions [23,24]. In Ref. [11] S_{ct} was not factorised out of the breakup amplitude but since the results obtained both for the core momentum distribution and the neutron breakup cross section are consistent with those of Ref. [12] and with the results we present in this paper, the authors of [11] conclude that the factorised form is a good approximation [25].

The effect of $|S_{ct}|^2$ in the integral in Eq.(2.6) is to cut-off small values of the core-target impact parameters. In Ref. [22] we used a parametrized form for $|S_{ct}|^2$ which corresponds to a smooth cut-off in d . The effect of the smooth cut-off depends on the parameter η defined above. In the case of weak initial binding energy η is very small and the smooth cut-off correction is negligible as compared to a sharp cut-off. Furthermore in a recent paper [15] it has been shown that the breakup probability as a function of the core-target impact parameter, corresponding to $P(\varepsilon_f,d)P_{el}(d)$ in our formalism, is peaked at a radius quite larger than the sum of the projectile-target radii and it rises sharply from zero to the maximum value (cf.Fig.2 of [15]). In [15] a DWBA approach has been used, which takes into account properly the distortion of the relative motion trajectory by the core-target optical potential.

The above discussion justifies the use of a sharp cut-off in d. Thus a simple expression for the cross section is obtained, which is valid when P_{el} is given by the strong absorption model such that $P_{el} = 1$ if $d \geq R_s$ $P_{el} = 0$ if $d < R_s$ [21],

$$\frac{d\sigma}{d\varepsilon_f} \approx C^2 S\frac{\pi R_s}{\eta}\left(1+\frac{1}{2\eta R_s}\right)\frac{dP(R_s)}{d\varepsilon_f}. \tag{2.7}$$

The above equation is consistent to leading order in $\frac{1}{\eta}$ with the formulae given in [12] for $l_i = 0, 1$. Eq.(2.4) is also similar to the breakup probability of [12] where instead of the

Glauber elastic plus absorption cross section factor the experimental neutron-target reaction cross section was used. The breakup cross section is sensitive to the choice of the strong absorption radius R_s [24,26,27]. It can be estimated from

$$R_s = 1.4(A_t^{1/3} + A_{pc}^{1/3}) \text{ fm}. \tag{2.8}$$

where A_t and A_{pc} are the mass numbers of the target and projectile core.

The momentum distribution is one factor in the breakup probabilities expressions Eq.(2.2) and (2.4) but there are other factors which combine to modify its relation with the cross section Eq.(2.7). One is the effect of the neutron-target rescattering shown explicitly by the Glauber factors of Eq.(2.4). Another is the η dependence in the factor $\frac{\pi R_s}{\eta}\left(1 + \frac{1}{2\eta R_s}\right)$ in Eq.(2.7) coming from the ion-ion scattering and giving a kind of modified nucleus-nucleus geometrical cross section.

The incident energy dependence in the total breakup probability is contained mainly in the neutron-target phase-shift δ_{l_f}, as shown explicitly by the Glauber form $\chi(\mathbf{b}) \approx \tilde{V_2}(\mathbf{b}, 0)/(v\hbar)$. This is partly because of the factor $1/v$ in the expression for $\chi(\mathbf{b})$ but also because the neutron-target optical potential V_2 is energy dependent. However as we mentioned after Eq.(2.4) the energy distribution of the final neutron has its main origin in the k_1 dependence of $\tilde{\psi}_1(d, k_1)$, the momentum distribution of the neutron in the initial state. With the approximate form Eq.(2.5) it is contained mainly in the factor $\exp(-2\eta d)$.

III. APPLICATION TO ^{11}BE BREAKUP

The situation is especially striking for breakup of a halo nucleus like ^{11}Be where the binding energy $\varepsilon_i = -0.5MeV$ of the neutron in the initial nucleus is very small. The factor $\exp(-2\eta d)$ has a sharp maximum when $\eta = \gamma_i = 0.155fm^{-1}$ or $k_1 = 0$ and $\varepsilon_f \approx mv^2/2$. The small value of γ_i gives distributions in k_1 which are sharper than those obtained for normal heavy ions where the initial binding energy is of the order of $-10MeV$ and it makes the breakup cross section large. The values of η as a function of the neutron final energy ε_f are shown in Fig.(1a) for the case of ^{11}Be by the solid line. Also shown is the same parameter for a ^{10}Be projectile (dot line) whose neutron separation energy is $\varepsilon_i = -6.8MeV$ and $l_i = 1$. There is a much stronger energy dependence and the minimum value of η is much smaller in the case of ^{11}Be. The corresponding k_1-dependence of $\tilde{\psi}_1$, calculated from Eqs.(2.5) is shown in Fig.(1b). As expected the momentum distribution is sharper in ^{11}Be (solid line) than in ^{10}Be (dashed line). It is also a characteristic of an s-state momentum distribution to be narrower than for p-states, d-states or larger l-values.

The initial state amplitude $\tilde{\psi}_1(d, k_1)$ depends on the choice of $d = R_s$ which in Fig.(1b) was taken to be $6.2fm$ and which is appropriate for the breakup reaction of ^{11}Be on a ^9Be target. For a ^{208}Pb target we take $R_s = 11.5fm$. These are close to values given by Eq.(2.8). The widths at half maximum of the resulting momentum distributions are $\hbar\Delta k_1 = 49MeV/c$ for a ^9Be target and $\hbar\Delta k_1 = 39.4MeV/c$ for a ^{208}Pb target. The difference is due to the change in the strong absorption radius. The dependence of the parallel momentum distribution on d or equivalently on R_s can be understood by noting that the parallel momentum distribution Eq.(2.5) is such that the square of its modulus represents the probability of finding a neutron in the projectile with a certain value of its momentum parallel to the relative motion velocity, when it is at a definite distance d from the center of the initial nucleus.

The next step is to discuss whether information about the width of the neutron momentum distribution in the initial nucleus can be obtained from the breakup spectra. To be specific we focus on breakup reactions with a ^{11}Be projectile on two targets. One possibility would be to use the measured spectra of breakup neutrons. In fact most of the present experiments use the energy loss spectra of the ^{10}Be fragments. If elastic breakup is the only mechanism leading to ^{10}Be fragments these two approaches would be equivalent. By energy conservation, Eq.(2.1), the ^{10}Be energy loss spectra would have the same shape as the neutron spectra of Fig.(2). On the other hand the absorption component of Eqs.(2.2) and (2.4) refers to neutrons which are detached from the projectile and are either inelastically scattered or cause some reactions in the target. They would have their energy degraded or might not been seen at all, but the energy loss spectrum of the ejectile can still be measured. In the figures the spectra are plotted as a function of ε_f, but they can be interpreted as energy loss spectra using equation (2.1).

In Fig.(2) we show the energy spectra for the reaction $^9Be(^{11}Be,^{10}Be)^9Be + n$ at $E_{inc} = 10$, 41 and $72A.MeV$ calculated according to Eq.(2.2) with an optical model S-matrix. The optical potential used is from [28]. Technical details concerning this kind of calculations can be found in Refs. [17,18]. For the $2s_{1/2}$ initial state in ^{11}Be the parameters appearing in Eqs.(2.5) and (2.7) are: the spectroscopic factor $C^2S = 0.77$, and the asymptotic normalization constant $C_1 = 0.94fm^{-1/2}$. The dot lines in Fig.(2) are the elastic breakup spectra while the dashed lines are the absorption spectra. The solid lines give their sum which correspond to the ejectile inclusive energy spectra leading to ^{10}Be fragments. The relationship between the momentum scale in Fig.(1b) and the energy scale in Fig.(2) is contained in the definition of k_1 given after Eq.(2.3). In the same way the neutron parallel momentum distribution after breakup can be obtained from Eq.(2.7) by a simple change of variable from ε_f to k_1. Thus the simple expectation is that the width $\Delta\varepsilon_f$ of the neutron energy spectrum should be related to the width $\hbar\Delta k_1$ of the halo neutron momentum distribution by

$$\hbar\Delta k_1 = \Delta\varepsilon_f / v. \tag{3.1}$$

However because of the extra factors in Eq.(2.7) there is a modification in the above relation. To show the extent of the modification Table I gives values of $\hbar\Delta k_1$ obtained from the calculated energy spectra using the relation (3.1) for a ^9Be target and a ^{208}Pb target. The optical potentials used were from [28] and [29] respectively. In each column the first number refers to ^{208}Pb and the second to ^9Be . The numbers in the last column should be compared with the widths of the momentum distribution Eq.(2.5), which is $\hbar\Delta k_1 = 39.4MeV/c$ for the ^{208}Pb target, because $R_s = 11.5$ and $\hbar\Delta k_1 = 49MeV/c$ for the ^9Be target from Fig.(1b), where $R_s = 6.2$. In the case of Pb there is a close correspondence between the width of the calculated energy distribution and the width of the momentum distribution Δk_1. On the other hand the values of Δk_1 extracted from the energy distribution for the Be target are 20% smaller than the Δk_1 from Fig.(1b).

To show this effect more clearly we have plotted in Fig.(3a) the differential cross section or energy spectra as a function of k_1, at the same incident energies as Fig.(2). Diamonds, dot line and crosses are for $E_{inc} = 10$, 41, $72 A.MeV$ respectively. The full line is the initial momentum distribution in ^{11}Be as in Fig.(1b). All curves are normalized at the same peak value. Fig.(3a) is for the Be target and one can see that the initial momentum distribution is wider than the values obtained from the energy spectra. For a Pb target instead, Fig.(3b) shows that the energy spectra at high energy reproduce well the initial momentum distribution width. The different scales in Figs.(3a) and (3b) reflect the difference in $\tilde{\psi}_1(d, k_1)$ when d changes. One possible reason for this behaviour is the fact that in the case of the Pb target the halo wave function is probed at a larger distance as compared to the Be case. Thus changing the target but keeping the incident energy fixed on can get information on the momentum distribution at different radii.

Results which seem consistent with our discussion have been obtained by Kelley et al. [30] who measured the parallel momentum distribution of ^{10}Be fragments on several targets. They found $\Delta k_1 = 41.6 \pm 2.1 MeV/c$ on a Be target, in agreement with our value in Table I. Also their results show a 5% change in the widths depending on the target, again in agreement with the maximum variation shown by our calculations. A similar target dependence was remarked in [31] in connection with ^{11}Li data. On the other hand the small Δk_1 values obtained at low incident energies for the same targets are due to the fact that because of the relation between k_1 and ε_f the tails of the momentum distributions in Fig.(1b) cannot be sampled by a low energy reaction.

In the case of a heavy target the experimental spectra contain an important contribution from Coulomb breakup which we discuss in [32]. Here we anticipate that for the lead target the Coulomb breakup calculated spectra give $\hbar\Delta k_1 = 43MeV/c$ and $47MeV/c$ at $E_{inc} = 110MeV$ and $790MeV$ respectively.

Widths calculated from the energy distributions obtained with the eikonal model Eq.(2.4) are about 10% smaller than the ones given in Table I obtained with an optical model final wave function using the more accurate energy distribution in Eq.(2.2). The agreement between the two calculations improves increasing the incident energy and for heavy targets. However the absorption is always underestimated by the eikonal approximation. This is because the contribution from the very low partial waves which is correctly described by the optical modes S-matrix in Eq.(2.2) is instead underestimated by the eikonal S-matrix. Elastic breakup is dominated by high partial waves which are well described by the eikonal S-matrix. In this respect it can be useful to remark that while for a light target partial waves up to $l_f = 7$ are enough to describe the neutron rescattering on the target, in the case of the Pb target we found that partial waves up to $l_f = 25$ have to be taken into account. This is possible and easy to do with the present method while it requires very cumbersome calculations in other methods like DWBA.

The relative amount of nuclear vs. Coulomb breakup in the total breakup cross section, for heavy targets is currently a question of debate for the experimental and theoretical implications [33]. In the case of heavy targets we are studying the important contribution to the exclusive cross sections from Coulomb breakup in [32]. The results could be used to disentangle the two mechanisms. Therefore we give in Table II the calculated cross sections integrated over energies and angles, for the breakup of ^{11}Be on ^{9}Be, ^{48}Ti and ^{197}Au

[34] at $E_{inc} = 41A.MeV$ and on a ${}^{208}Pb$ target [35] at $E_{inc} = 72A.MeV$ together with the experimental values for the inclusive and exclusive cross sections. The first row gives experimental and theoretical values for inclusive cross sections. The theoretical values are the sum of the elastic, Coulomb and inelastic contributions, given in the third to fifth rows. The second row gives the exclusive values. In this case the theoretical estimates are the sum of the Coulomb and nuclear elastic cross sections. The Coulomb breakup calculations [32] were done in first order perturbation theory similarly to [34]. Our results agree well with experimental values and with other theoretical estimates [34,36] and show that for heavy targets the nuclear breakup, although smaller than the Coulomb breakup, cannot be considered negligible. The cross section for the lead target are slightly smaller than those for the gold target because the incident energy was higher.

Our results for the reaction ${}^{9}Be({}^{11}Be,{}^{10}Be){}^{9}Be + n$ were obtained with $R_s = 6.2fm$. Using $R_s = 5.9fm$ gives $\sigma_{breakup} = 0.41b$ while using $R_s = 6.5fm$ gives $\sigma_{breakup} = 0.36b$. For comparison, the results for the neutron breakup from the ${}^{10}Be$ core at $R_s = 6.2fm$ are: $\sigma^{el} = 0.025b$ and $\sigma^{inel} = 0.037b$, where we assumed a spectroscopic factor $C^2S = 4$ for the $1p_{3/2}$ state in ${}^{10}Be$. Since the experimental spectroscopic factor is in fact 2.1 and the rest of the occupation probability is spread over three excited bound states in ${}^{10}Be$, the above value can be considered as a higher limit estimate for the core breakup contribution at $E_{inc} = 41A.MeV$. The elastic plus inelastic cross sections obtained using the eikonal formula (2.4) are smaller by about 25%. This is mainly due to the absorption term for which the eikonal approximation is not very accurate. Here and in the following we refer to the cross section coming from the absorptive term of Eq.(2.2) as inelastic.

At this point it is worth mentioning that some authors [11,12] refer to the absorptive term as to stripping, while others [13] have used the term inelastic breakup to include also processes in which the core nucleus interacts inelastically with the target, besides those discussed here which are due to the neutron-target interaction. However as it has been discussed in [13] these processes are expected to give rise to a small core survival probability and therefore they have often been neglected. Since it is always the $(A_p - 1)$ nucleus which is detected, its possible excitations must be restricted to those below particle threshold. We have discussed and included such processes in our calculations for breakup of normal nuclei [18,20] and the same can be done for halo projectiles. The values of cross sections for the core breakup given above give an estimate of such processes. Some experimental evidence for such reactions has recently been discussed by Hansen [37].

In view of future experiments in the incident energy range $3 - 10A.MeV$ it is useful to know the energy dependence of the nuclear elastic and inelastic total breakup cross section. In Fig.(4a) we show the total elastic (cross) and inelastic (star) cross sections and the sum (diamond) of them for a ${}^{9}Be$ target. They have been obtained from the integration of the energy spectra from Eqs.(2.2) and (2.7) calculated at different incident energy. The very interesting point is the relative behaviour at low energy of the two components of the breakup and also the dependence on the target. For this reason we show also in Figs.(4b) and (4c) the cross section values calculated for a ${}^{28}Si$ [38] and a ${}^{208}Pb$ [35] target. The neutron optical potentials used are from [28,39,29] respectively, for the three targets. Comparing the three cases we notice that at high incident energies the elastic and inelastic breakup tend to give the same cross section. This is the geometric limit of the nuclear cross section.

At low energies in the case of the light target ${}^9Be$ the elastic breakup is larger than the inelastic one and this pattern is maintained increasing the incident energy. This is because the neutron-light-target optical potentials have only a surface component of the imaginary part, due to the fact that these nuclei can have surface collective excitations but do not have enough density of levels to allow the absorption into compound nucleus. On the other hand in the case of ${}^{208}Pb$ the absorption is larger at all energies because there is a large probability of surface excitations leading to neutron inelastic breakup and also to the fact that the neutron-Pb optical potential has a volume term of almost constant magnitude at high energies. Our results are consistent with those of [11,12] in the case of the Be target.

IV. CONCLUSIONS

To conclude, neutron breakup from the projectile in a heavy-ion reaction has been discussed in this paper in the framework of the theory of transfer to the continuum reactions which uses an optical model final state wave function for the neutron and the relation with the eikonal model has been clarified. The latter is a good guideline to understand the mechanism of halo breakup and it is quite accurate to describe the halo neutron breakup at high incident energy and on a heavy target. In other situations one should use Eq.(2.2) with an optical model S-matrix. Both methods can be used to calculate energy spectra but the angular distributions of the breakup neutron can be obtained only from the eikonal model [21] which contains the explicit dependence on the neutron final momentum components, furthermore this method can be easily extended to relativistic energies, as it has been done in [11].

The models have been applied to the breakup of ${}^{11}Be$ on several target nuclei. The neutron energy distribution has a peak centered at the incident energy per nucleon of the ${}^{11}Be$ projectile with a width related to the width of the momentum distribution of the halo neutron. To a first approximation there is a very simple relation between these two widths, but sample calculations show that, due to details of the reaction mechanism, there can be differences between the initial momentum distribution and the measured one which can reduce its original widths up to 20% for a light target nucleus.

Integrated nuclear elastic and inelastic breakup cross sections have been calculated and compared to experimental values and to Coulomb breakup cross sections. In the case of heavy targets it is very important to estimate the two contributions separately. Our results agree well with experimental values and show that for heavy targets the nuclear breakup, although smaller than the Coulomb breakup, cannot be considered negligible. Finaly the incident energy dependence of the nuclear elastic, inelastic and total cross section has been studied.

We are grateful to P.G.Hansen for comments on an early version of this paper and to G.F. Bertsch for discussions. One of us (A.B.) wishes to thank W.Tornow for discussions and for information on neutron-light-nucleus optical potentials and H.Horiuchi for the hospitality in Kyoto during the preparation of this paper.

REFERENCES

[1] R. Serber, Phys. Rev. **72**, 1008 (1947).

[2] R. J. Glauber, Phys. Rev. **99**, 1515 (1955).

[3] J. Hüfner and M. C. Nemes, Phys. Rev. C **23**, 2538 (1982).

[4] C. A. Bertulani and K. W. Mc Voy, Phys. Rev. C **46**, 2638 (1992).

[5] Y. Ogawa, K. Yabana, and Y. Suzuki, Nucl. Phys. **A543** (1992) 722.

[6] F. Barranco, E. Vigezzi and R. A. Broglia, Phys. Lett. B **319**, 387 (1993).

[7] H. Sagawa and N. Takigawa, Phys. Rev. C **50**, 985 (1994) .

[8] A. A. Korsheninnikov and T. Kobayashi , Nucl. Phys. **A576**, (1994) 97.

[9] P. G. Hansen, Nucl. Phys. **A588**, 1c (1995).

[10] H. Esbensen, Phys. Rev. C **53**, 2007, (1996).

[11] K. Hencken, G.F. Bertsch and H. Esbensen, Phys. Rev. C **54**, 3043, (1996).

[12] P. G. Hansen , Phys. Rev. Lett. 77, 1016 (1996).

[13] Y.Ogawa and I.Tanihata, Nucl. Phys.**A616**, 239c (1997).

[14] G.F. Bertsch, K. Hencken and H. Esbensen, Phys. Rev. C **57**, 1366, (1998).

[15] R. Shyam and H. Lenske, Phys. Rev. C **57**, 2427, (1998).

[16] A. Bonaccorso and D. M. Brink, Phys. Rev. C **38**, 1776 (1988).

[17] A. Bonaccorso and D. M. Brink, Phys. Rev. C **43**, 299 (1991).

[18] A. Bonaccorso and D. M. Brink, Phys. Rev. C **44**, 1559 (1991).

[19] A. Bonaccorso and D. M. Brink, Phys. Rev. C **46**, 700 (1992).

[20] A. Bonaccorso, I. Lhenry and T. Süomijarvi, Phys. Rev. C **49** , 329 (1994).

[21] A. Bonaccorso and D. M. Brink, Phys. Rev. C **57**, R22 (1998).

[22] A. Bonaccorso, D. M. Brink and L. Lo Monaco, J. Phys. G13, 1407 (1987).

[23] R. A. Broglia and A. Winther, "Heavy Ion Reactions: Lecture Notes", 2nd Edition, Addison-Wesley, Redwood City, Calif. 1991.

[24] R. Bass, *Nuclear Reactions with Heavy Ions*, Springer-Verlag, Berlin 1980. Secs. 3.3 and 4.2.

[25] G. F. Bertsch, private communication.

[26] D. M. Brink, *Semiclassical Methods in Nucleus-Nucleus Scattering*, Cambridge University Press, Cambridge, 1985. Pag. 19.

[27] G. R. Satchler, *Direct Nuclear Reactions*, Clarendon Press, Oxford 1983. Pag. 529.

[28] J. H. Dave and C. R. Gould, Phys. Rev. C **28**, 2212 (1983).

[29] C. Mahaux and R. Sartor, Adv. Nucl. Phys. **20**, 1 (1991).

[30] J. K. Kelley, Sam M. Austin, R. A. Kryger, D. J. Morrissey, N. A. Orr, B. M. Sherrill , M. Thoennessen, J. S. Wienfield, J. A. Winger and B. M. Young, Phys. Rev. Lett.**74**, 30 (1995).

[31] P. G. Hansen, A. S. Jensen, and B. Jonson, Ann. Rev. Nucl. Part. Sci. **45**, 591 (1995).

[32] J. Margueron, A. Bonaccorso and D.M.Brink, in preparation.

[33] C. H. Dasso, S. M. Lenzi and A. Vitturi, Nucl. Phys. **A611**, 124 (1996)

[34] R. Anne et al., Nucl. Phys. **A575**, 125 (1994).

[35] T. Nakamura et al., Phys. Lett. B **331**, 296 (1994).

[36] P. Banerjee, J. A. Tostevin and I. J. Thompson, SCNP-97/16 report.

[37] P. G. Hansen, Proccedings of the Topical Conference on Giant Resonances, Varenna 1998, to be published in Nucl. Phys. **A**.

[38] F. Negoita et al., Preprint Ganil 97-23.
[39] M. A. Al-Ohali, C. R. Howell, W. Tornow and R. L. Walter, AIP Conference Proceedings 339, E. J. Stephenson and S. E. Vigdor Editors, AIP Press,Woodbury, NY, pag.593, (1994).

Table I: Parallel momentum distribution widths for Be and Pb targets. The value of $\hbar v$ is related to the incident energy but takes into account the effect of the nucleus-nucleus Coulomb barrier at R_s

E_{inc} (MeV)	$\Delta\varepsilon_f$ (MeV)	$\hbar v$ (MeV $\cdot$ fm)	$\hbar\Delta k_1$ (MeV/c)
110	4.4 5.0	22.45 27.71	38.6 35.5
300	8.8 9.0	44.03 46.92	39.3 37.8
790	15.0 15.5	75.1 76.82	39.3 39.8
Target	Pb Be	Pb Be	Pb Be

Table II: Cross sections for Be, Ti, Au [34] and Pb [35] targets. The first row gives experimental and theoretical values for inclusive cross sections. The theoretical values are the sum of the elastic, Coulomb and inelastic contributions, given in the third to fifth rows. The second row gives the exclusive values. In this case the theoretical estimates are the sum of the Coulomb and nuclear elastic cross sections.

$\sigma(b)$	Be	Ti	Au	Pb
$(^{11}Be,^{10}Be)$	0.29 ± 0.04 0.39b	0.65 ± 09 0.70	2.45 ± 0.20 2.73	—- 2.39
$(^{11}Be,^{10}Be + n)$	0.24 ± 0.05 0.23	0.55 ± 0.11 0.47	2.5 ± 0.5 2.37	1.8 ± 0.4 2.09
el	0.22	0.28	0.35	0.3
$Coul$	0.0074	0.19	2.02	1.79
$inel$	0.16	0.234	0.39	0.3

Figure Captions

Fig.1.(a) Values of the parameter η from for ^{11}Be solid line, and ^{10}Be dot line. (b) Initial momentum distribution for the $2s_{1/2}$ state in ^{11}Be, solid line, and $1p_{1/2}$-state in ^{10}Be, dot line.

Fig.2. Final energy spectra from Eq.(2.7) for $^{9}Be(^{11}Be,^{10}Be)^{9}Be+n$ at $E_{inc}=10$, 41, $72A.MeV$. Dot lines are for elastic breakup, dashed lines for inelastic breakup and solid lines are their sum corresponding to the inclusive ^{10}Be spectrum via Eq.(2.1).

Fig.3 (a). Final energy spectra as a function of k_1, at the same incident energies as Fig.(2). Diamonds, dot line and crosses are for $E_{inc}=10$, 41, $72A.MeV$ respectively. Solid line is the initial momentum distribution as in Fig.(1b). All curves are normalized at the some peak value. (b) The same as Fig.(3a) for $^{208}Pb(^{11}Be,^{10}Be)^{208}Pb+n$.

Fig.4 Incident energy dependence of the breakup cross sections on ^{9}Be (4a),^{28}Si (4b) and ^{208}Pb (4c). Diamonds joined by full lines give the total breakup cross sections. Crosses with dot lines are for the elastic breakup while stars with dotdashed lines are the inelastic breakup cross sections.

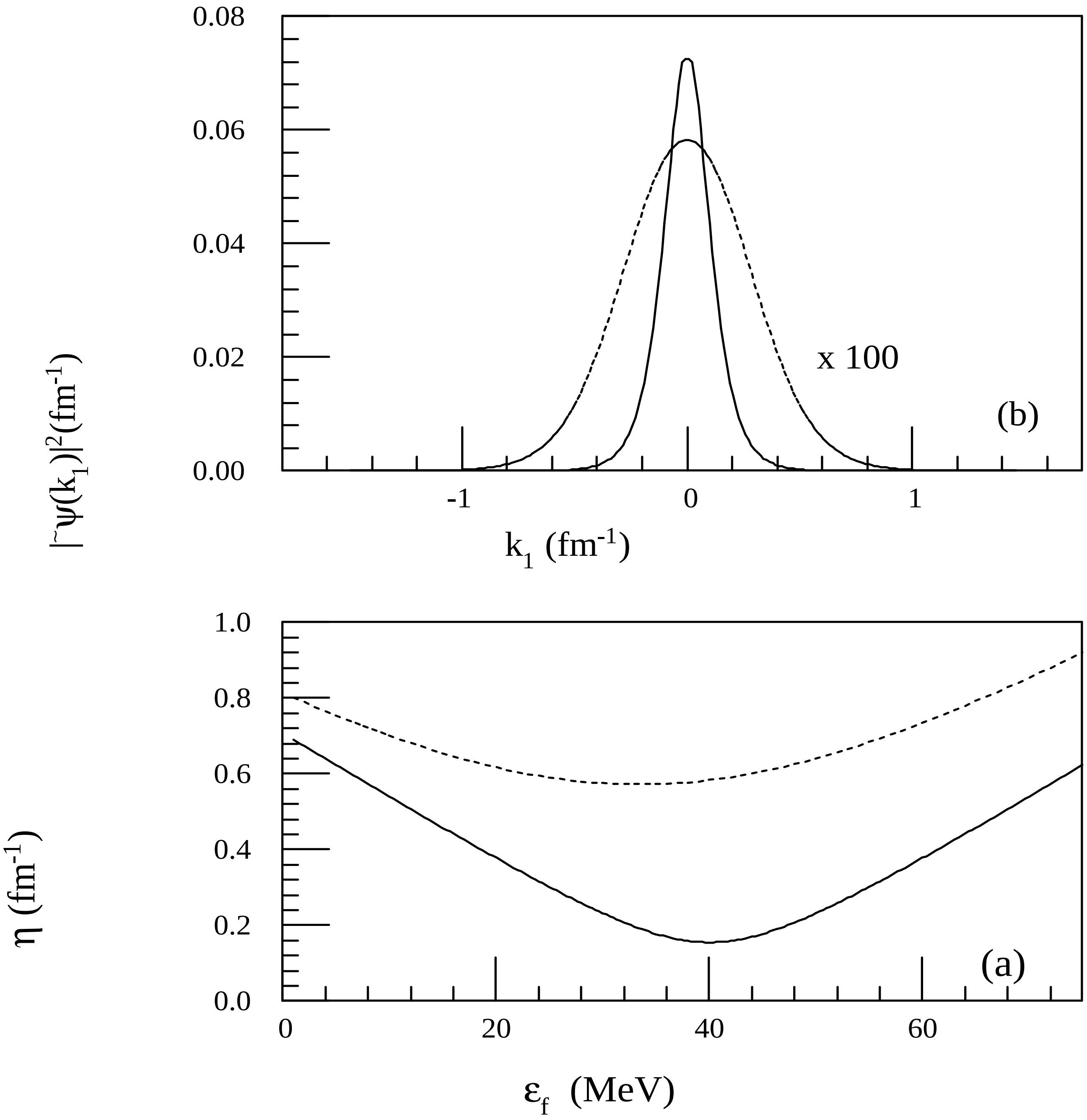

$|\tilde{\psi}(k_1)|^2 (\mathrm{fm}^{-1})$
0.08
0.06
0.04
0.02
0.00
x 100
(b)
-1
0
1
k_1 (fm^{-1})
η (fm^{-1})
1.0
0.8
0.6
0.4
0.2
0.0
(a)
0
20
40
60
ε_f (MeV)

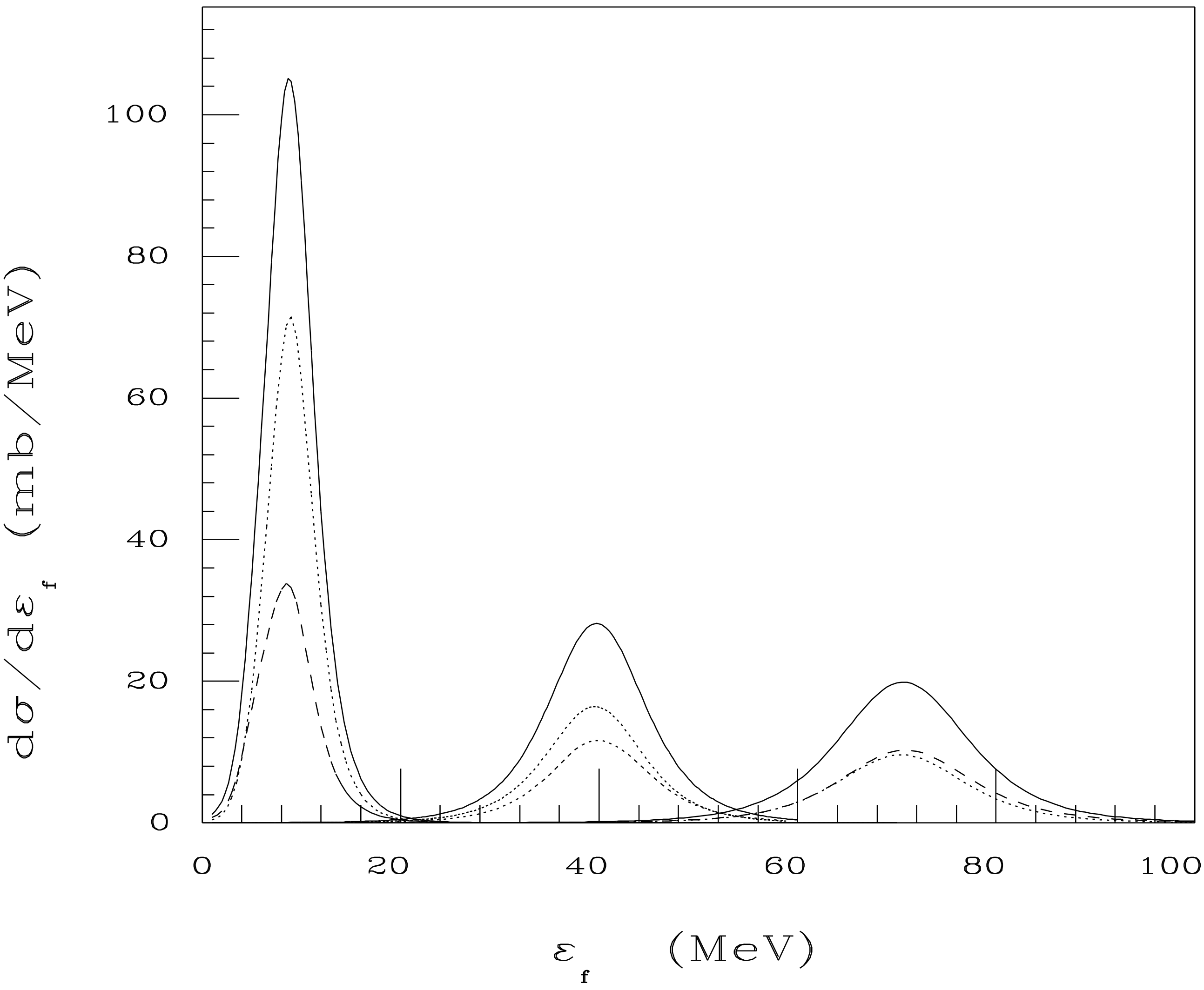

$d\sigma/d\varepsilon_f$ (mb/MeV)
0
20
40
60
80
100
ε_f (MeV)

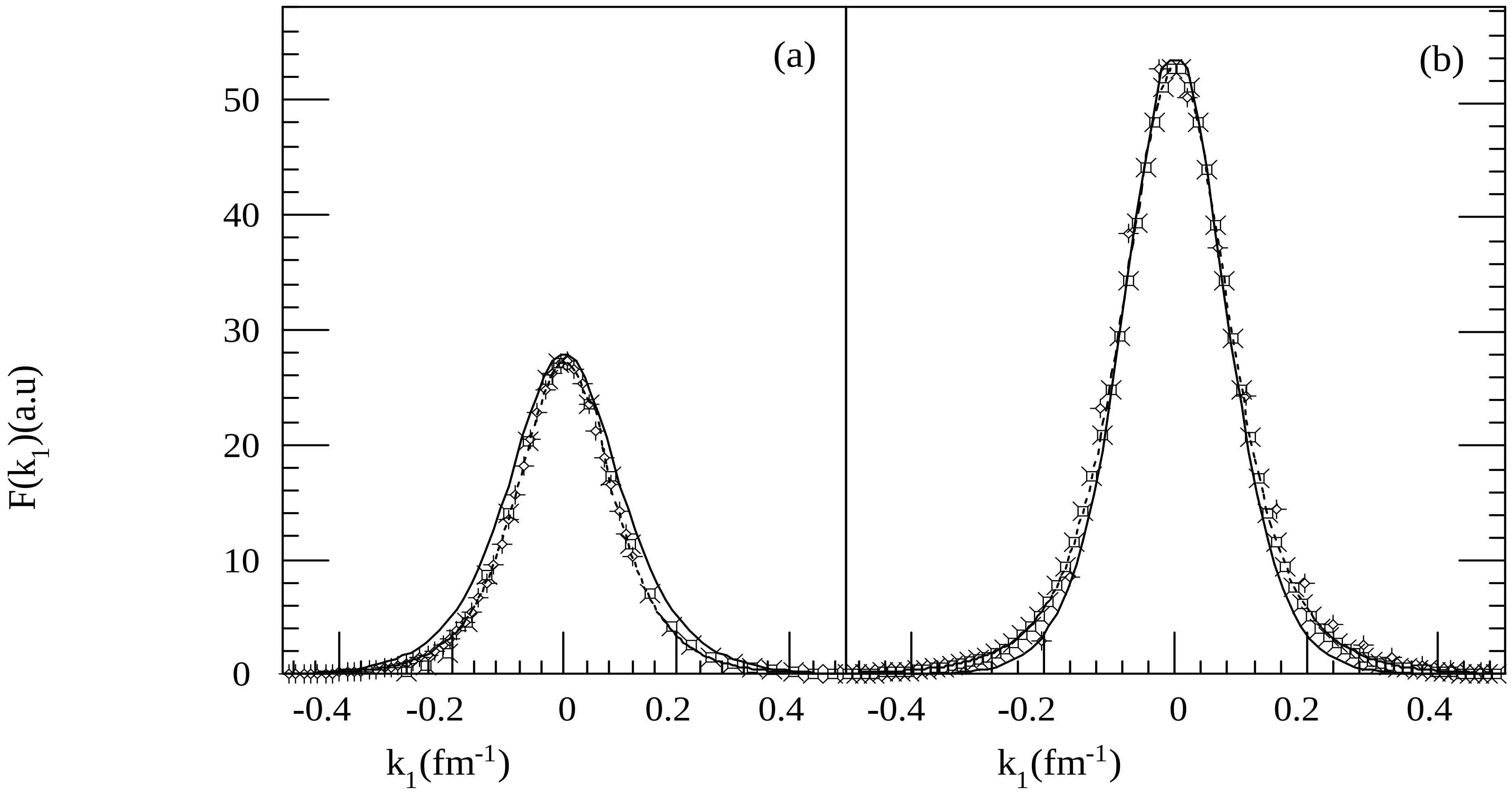
(a)
(b)
F(k$_1$)(a.u)
k$_1$(fm^{-1})
k$_1$(fm^{-1})
0
10
20
30
40
50
-0.4
-0.2
0
0.2
0.4

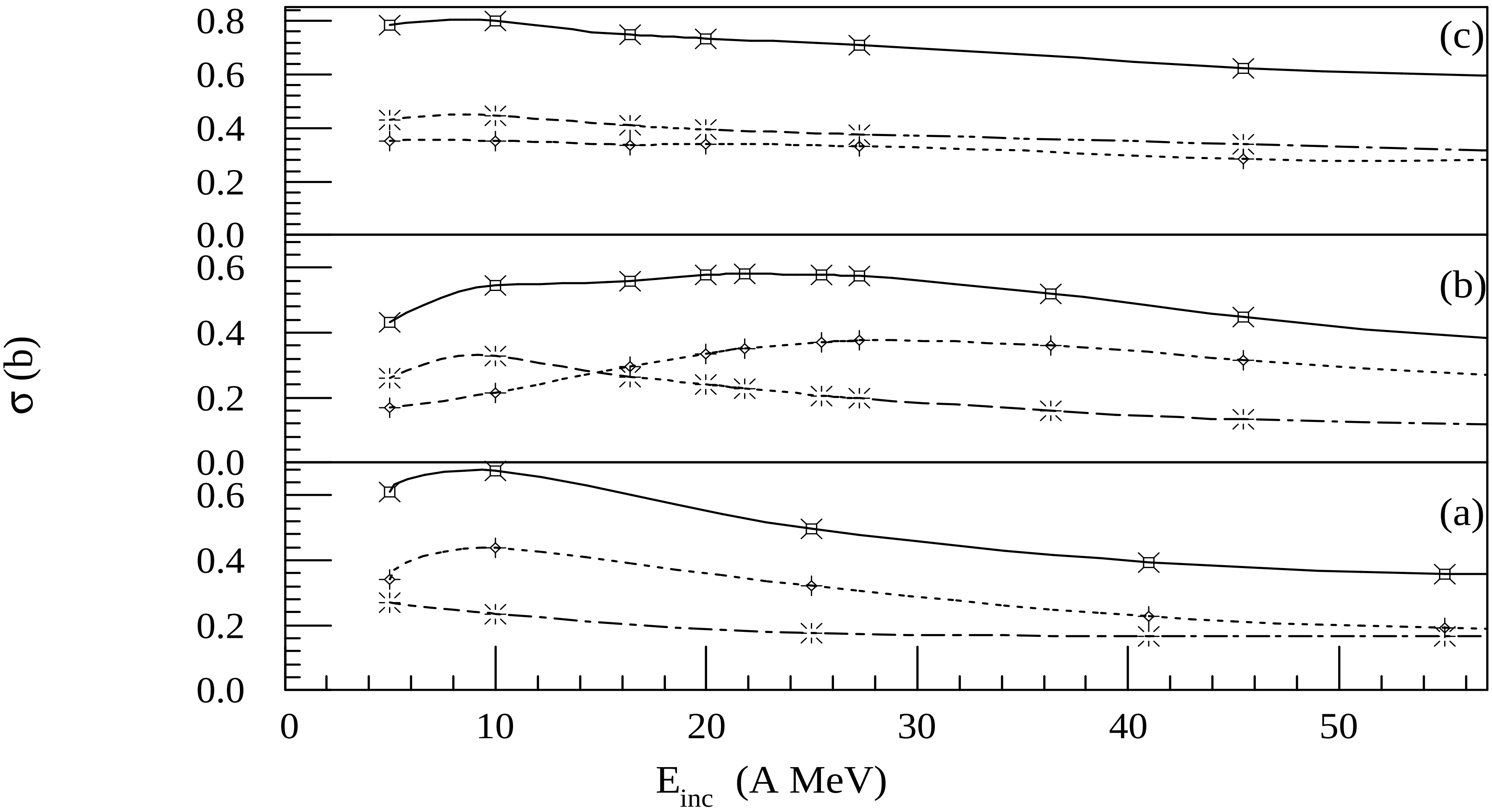
σ (b)
0.8
0.6
0.4
0.2
0.0
(c)
0.6
0.4
0.2
0.0
(b)
0.6
0.4
0.2
0.0
(a)
0
10
20
30
40
50
E_{inc} (A MeV)